lubricants

Article

The Impact of Lubricant Film Thickness and Ball Bearings Failures †

Matthew David Marko

Naval Air Warfare Center Aircraft Division, Joint-Base McGuire-Dix-Lakehurst, Lakehurst, NJ 08733, USA; matthew.marko@navy.mil

† NAVAIR Public Release 2018-609 Distribution Statement A—"Approved for public release; distribution is unlimited".

Received: 14 February 2019; Accepted: 30 May 2019; Published: 2 June 2019

Abstract: An effort was made to find a relationship between the lubricant thickness at the point of contact of rolling element ball bearings, and empirical equations to predict the life for bearings under constant motion. Two independent failure mechanisms were considered, fatigue failure and lubricant failure resulting in seizing of the roller bearing. A theoretical formula for both methods was established for the combined probability of failure using both failure mechanisms. Fatigue failure was modeled with the empirical equations of Lundberg and Palmgren and standardized in DIN/ISO281. The seizure failure, which this effort sought to investigate, was predicted using Greenwood and Williamson's theories on surface roughness and asperities during lubricated contact. These two mechanisms were combined, and compared to predicted cycle lives of commercial roller bearing, and a clear correlation was demonstrated. This effort demonstrated that the Greenwood–Williams theories on the relative height of asperities versus lubricant film thickness can be used to predict the probability of a lubricant failure resulting in a roller bearing seizing during use.

Keywords: lubrication; ball bearings; roller bearings; failures; film thickness

1. Introduction

Ball bearings are used in countless mechanical applications to convert sliding mechanical contact into rolling contact [1–3], dramatically reducing friction energy losses. Sliding contact inherently has a high friction force, as random asperities can contact the surface and induce wear and damage to machined parts [4–9]. Rolling contact, however, has dramatically lower friction; the overwhelming majority of the friction loss is merely hysteresis from elastic deflections of the circular bearings.

Rolling element bearings are one of the most common configuration of ball bearings, with the bearings contained in a circular race to allow continued circular motion. As long as there is a minimum surface friction to enable the bearings to roll, there will be a dramatic reduction in circular friction for an object spinning inside or outside of the races. Bearings can be spherical, cylindrical, or a host of different configurations depending on the applications of the ball bearings.

A well built bearing can last indefinitely, however all mechanical objects have some risk of failure. Despite the previous assumptions that stresses less than half of yield have no significant risk of failure, there is always some risk of fatigue and fracture, which may manifest itself in the life of a ball bearing. The most likely bearing failure, however, is lubricant failure causing the bearings to seize. Ball bearings overwhelmingly use lubricant oils and greases to ensure there is not an excessive build-up of heat and friction between the races and the bearings. While a minimum amount of friction is necessary to ensure the bearings roll rather than slide (often specified as a minimum axial load), too much friction can cause the bearings to stick to the race and seize up, rather than allowing rolling.

Friction is inherently random and variable, as it is impacted by the different random surface asperities; as such, it is incredibly difficult to model. The usual (but not exclusive) mechanism of lubricant failure is as follows: a high enough friction will heat the lubricant, which will reduce the viscosity of the lubricant, which will increase the friction heating, and this feedback loop will continue until the friction between the bearing and the races is so great that the bearing seizes. If a bearing seizes during a critical application, the results can be catastrophic.

While it is impossible to truly know the exact nature of every bearing surface, empirical equations can be generated to determine the L_{10} life from a known bearing load, lubricant cleanliness, lubricant viscosity, and continuous bearing speed. The L_{10} life is defined as the number of revolutions a bearing can experience before a 10% chance of bearing failure. This effort was to study how tribological properties such as the lubricant film thickness [10–12] can serve to predict the change of failure after a single revolution, and thus estimate the L_{10} life.

2. Empirical Equations for L_{10} Life

To properly develop a numerical model for ball bearing failures, it is necessary to have empirical data on bearing failure to verify and validate it. In this aim, the L_{10} empirical equations provided by Timken [13] was used as a basis for validating predictions of bearing life as a function of lubricant thickness. The world's largest manufacturer of ball bearings is Svenska Kullagerfabriken (SKF), a Swedish company founded in 1907; they use a bearing life calculator [14,15] similar to Timken as well. Timken's life equations were provided in easily duplicated empirical equations, versus a software life calculator; for the purpose of this analysis, Timken was used. These Timken empirical equation ultimately yield the L_{10} life in revolutions before the bearings have a 10% chance of failure. The core equation for L_{10} life is [13]

$$L_{10} = A_{10} \cdot (\frac{C_{a1}}{P})^{\hat{p}} \cdot 10^6, \tag{1}$$

where C_{a1} (N) is the basic dynamic load rating, P (N) is the equivalent load, and A_{10} is the life modification factor. The value of $\hat{p}$ was found empirically, and it is 3 for spherical bearings and 10/3 for cylindrical bearings [16–18], based on empirical research of Lundberg and Palmgren [16–18].

The value of A_{10} is a function of several dimensionless parameters

$$A_{10} = a_1 \cdot a_2 \cdot C_g \cdot C_l \cdot C_j \cdot C_s \cdot C_v \cdot C_{gr}, \tag{2}$$

where a_2 is a material factor that was treated as 1 for steel bearings; C_g is a geometry factor set to 1 for spherical roller bearings; G_{gr} is the grease factor that is set to 1 if not using grease and 0.79 with grease; a_2 is a material factor set to 1 for steel bearings; and C_j ranges between 0.747 and 1.0, depending on how tapered the bearing is, and this simulation assumed $C_j = 1$ for non-tapered bearings. The value of C_l is inverse proportional to the equivalent load P (N)

$$\begin{aligned} C_l &= P^{-0.25}, \\ P &= F_a + 1.2 \cdot F_r, \end{aligned} \tag{3}$$

where F_a (N) and F_r (N) are the axial and radial loads. The speed factor is proportional to the square root of the speed in revolutions per minute

$$C_s = \sqrt{\Omega_{RPM}}, \tag{4}$$

and the viscosity factor C_v is proportional to the square root of the kinematic viscosity ν (cSt) in centistokes

$$C_v = 1.6 \cdot \sqrt{\nu}. \tag{5}$$

Finally, the factor a_1 is set to the probability of failure of interest,

$$a_1 = 4.26 \cdot (log \frac{100}{R})^{2/3} + 0.05, \tag{6}$$

where R represents the probability of surviving the calculated number of cycles. If R = *90*, to represent L_{10}, then the value of a_1 is 1.

3. Tribological Predictions of L_{10} Life

Equation (1) can predict the L_{10}, but it gives no information as to the mechanics of the failure; it is purely based on empirical data. To better understand the mechanism of failure, a model based on the tribological properties to find the values of L_{10} needs to be developed, with Equation (1) being used to verify and validate this model.

Regardless of the L_{10} life, a ball bearing failure can happen; L_{10} life is really a function of the probability of failure in the face of random conditions such as surface asperities. One common form of bearing failure is seizure, where excessive friction can yield increased heating, which reduces the lubricant viscosity, increasing the friction; eventually, the friction increases until it is high enough that the bearing seizes. Another potential cause of failure is a failure in fatigue; this increases exponentially with increasing load relative to fatigue life. For the purpose of the analysis, the driving cause of failure is treated as an excessively high increase in friction from the approximated average friction.

The greater the lubricant thickness is at the point of elastohydrodynamic contact, the less wear and friction can be expected. According to Greenwood and Williamson's research [19–24], wear and friction (other than from fluid stresses, and hysteresis of rolling contact) occur due to random asperities exceeding the thickness of the lubricant film [19–26]; the thicker is the lubricant, the lower is the mean ratio of true contact area ratio [1,27]. Assuming the surface asperities height follows a normal distribution, the ratio of metal-on-metal contact A_{real}/A with the lubricant thickness should roughly follow

$$\frac{A_{real}}{A} \approx exp(-\frac{h}{\sigma}), \tag{7}$$

where A_{real} (m^2) represents the true metal-on-metal contact area, A (m^2) represents the apparent (but not true) surface contact area, h (m) represents the lubricant film thickness, and σ (m) represents the RMS average asperities height. In addition to the fatigue life, where the failure life is proportional to the load over the fatigue load to the power of 10/3, it is expected that the L_{10} probability of lubricant failure will be a function of the lubricant film thickness h (m)

$$L_{10} = f(h) + f(\frac{C_{a1}}{P}) \tag{8}$$

4. First Parametric Study

The simulation assumed a lubricant with an ISO Viscosity Grade of 46, with a kinematic viscosity of 46 cSt at 40 °C, and kinematic viscosity of 8.5 cSt at 100 °C, lubricant properties of a typical commercially available bearing gear oil (*Mobil SHC 625*). The temperature range in the simulation was varied from 20 °C to 300 °C (112.2355 cSt to 1.0648 cSt). A copy of the Matlab computer code for this simulation is included in the Supplementary Materials.

A parametric study was conducted, utilizing the Timken 29348 roller bearing. This has an inner bore of 240 mm, a dynamic load rating C_{a1} of 2,040 kN, and an average roller diameter of 315.7 mm. While the roller diameters are not clearly specified, CAD estimation yielded a length of 49.68 mm and an average roller radius of 18.87 mm, with a total of 23 rollers. The bearing is made of steel, thus the Young's modulus E_Y is 210 GPa, and the Poisson's ratio p is 0.3. The parametric study calculated both the L_{10} life as defined in Equation (1), and compared it to the predicted lubricant film thickness [10–12,28–40], and the relative fatigue load. The parametric study was conducted for a temperature ranging between 20 °C and 300 °C, in increments of 10 °C; an equivalent axial load of 1–100% (in 1% increments) of the 2,040 kN dynamic load C_{a1}; and a bearing speed of 1,000–15,000 RPM, in increments of 500 RPM. With each of these parameters, the L_{10} life was calculated with Equation (1).

The next step was to predict the film thickness of the lubricant at the point of contact between the bearings and the rollers during elastohydrodynamic contact [1,41–48]. In 1974, empirical equations by Hamrock and Dowson [33] characterized the minimum h_0 (m) and central h_c (m) film thickness

$$h_{min} = 3.63R'(U_n^{0.68})(G_n^{0.49})(W_n^{-0.073})(1-exp[-0.68\kappa_{ellipse}]), \tag{9}$$

$$h_c = 2.69R'(U_n^{0.67})(G_n^{0.53})(W_n^{-0.067})(1-0.61\cdot exp[-0.73\kappa_{ellipse}]), \tag{10}$$

$$U_n = \frac{\mu_0 U}{E'R'}, \tag{11}$$

$$G_n = \alpha_{PVC}E', \tag{12}$$

$$W_n = \frac{W}{E'R'^2}, \tag{13}$$

where h_{min} (m) is the minimum film thickness, h_c (m) is the central film thickness, U_n is the dimensionless speed parameter, G_n is the dimensionless material parameter, W_n is the dimensionless load parameter, $\kappa_{ellipse}$ is the ellipticity of the contact area, μ_0 (Pa·s) is the dynamic viscosity of the lubricant at atmospheric pressure, and α_{PVC} (Pa^{-1}) is the pressure viscosity coefficient

$$\alpha_{PVC} = (0.965\cdot log_{10}(\nu)+0.6)\cdot 10^{-8}, \tag{14}$$

where ν is the kinematic viscosity (m^2/s) and U (m/s) is the velocity of contact. The reduced Young's modulus E' (Pa) and reduced radius R' (m) are for Hertz contact equations for elastic deflection [1,49]. Assuming cylindrical rollers and a consistent material were used, the equations for E' (Pa) and R' (m) are

$$R' = 1/\{\frac{1}{R_r}+\frac{1}{R_R}\}, \tag{15}$$

$$E' = \frac{E_Y}{1-p^2}. \tag{16}$$

where R_r (m) is the radius of the cylindrical bearing roller, R_R (m) is the radius of the bearing race, and E_Y (Pa) and p are the Young's modulus and Poisson's ratio of the bearing material.

To realize the minimum h_{min} and central h_c elastohydrodynamic film thickness, it is necessary to determine the dynamic viscosity of the lubricant. The viscosity of the lubricant, however, is affected by temperature [2,50–53], as hotter oils are inherently less viscous. A reduction in viscosity results in a reduced minimum film thickness [33], but this reduced film thickness results in a cooler oil film [29], as there is less thermal resistance from the center of the oil film to the surface of the ball bearing. As a result of this contradiction, it is necessary to use iteration to converge on a realistic lubricant oil temperature and viscosity, so that a minimum film thickness can be determined.

The first step is to calculate the flash temperature heating of the surface of the ball bearing. This is done by first calculating the dimensionless Peclet number [1,29]

$$L = \frac{U\cdot b_H}{2\alpha_{bb}}, \tag{17}$$

where b_H (m) is the length of contact, also defined as the Hertzian half width of the contact between the roller and the race [1]

$$b_H = \sqrt{\frac{4\cdot W\cdot R'}{\pi\cdot L_r\cdot E'_Y}}, \tag{18}$$

where L_r (m) is the half length of the roller, and α_{bb} (m^2/s) is the thermal diffusivity [54] of the ball bearing,

$$\alpha_{bb} = \frac{k_{bb}}{\rho_{bb} \cdot C_{P,bb}}, \tag{19}$$

where k_{bb} ($W/m^2 \cdot °C$) is the thermal conductivity, ρ_{bb} (kg/m^3) is the density, and $C_{P,bb}$ ($J/kg \cdot °C$) is the specific heat capacity; all of these $_{bb}$ parameters are for the ball bearing material (steel).

Once the dimensionless Peclet number L is known, one can calculate the average flash temperature [55–58], which is defined as the temperature that results from the high-pressure and heating. For $L < 0.1$, the friction heating is considered a *stationary* heat source, where the temperature distribution is effectively steady state, where the heat flow can be considered a flow of thermal current through a thermal resistance of the ball bearing. For $0.1 < L < 5.0$, the friction heating is considered a *slow-moving* heat source, where there is ample time for the temperature to be conducted through the ball bearing, and for $L > 5.0$ the friction heating is considered a *high-speed* heat source [29]. In this study, consistently the Peclet number has always exceeded the value of 5.

The predictive analytical equation used by this model for average flash temperature can vary with Peclet number, but the flash heating for Peclet numbers greater than 5 is [1,29]

$$\Delta T_F = \frac{0.266 \mu_{COF} \cdot W \cdot U}{k_{bb} \cdot b_H} \sqrt{\frac{\alpha_{bb}}{U \cdot b_H}} \quad L > 5.0, \tag{20}$$

where μ_{COF} is the dimensionless coefficient of friction (COF), b_H (m) is defined with Equation (18), W (N) is the load, and ΔT_F (°C) is the surface temperature increase due to friction. The value of μ_{COF} is assumed to be 0.0018, which is a standard friction coefficient for the rolling resistance spherical roller bearings [13–15].

The friction temperature can be used to calculate the average viscosity [1,45,46,53], where

$$\begin{aligned} \nu &= \hat{Z} - exp[-0.7487 - 3.295 \cdot \hat{Z} + 0.6119 \cdot \hat{Z}^2 - 0.3193 \cdot \hat{Z}^3], \\ \hat{Z} &= 10^\wedge[10^\wedge(A - B \cdot log_{10} T_L)] - 0.7 \end{aligned} \tag{21}$$

where ν (mm^2/s) is the kinematic viscosity, and A and B are dimensionless coefficients derived empirically. They can be found by measuring the kinematic viscosity at two temperature points, calculating the Z-value [53],

$$Z = \nu + 0.7 + exp[-1.47 - 1.84\nu - 0.51\nu^2], \tag{22}$$

and obtaining the viscosity coefficients, where [53]

$$\begin{aligned} log_{10} log_{10} Z &= A - B \cdot log_{10} T, \\ B &= \frac{log_{10} log_{10} Z_i - log_{10} log_{10} Z_j}{log_{10} T_j - log_{10} T_i}, \\ A &= log_{10} log_{10} Z_i + B \cdot log_{10} T_i, \end{aligned} \tag{23}$$

where T_i, T_j, Z_i, and Z_j are the temperature (Kelvin) and Z-coefficients at temperature points i and j. To convert the values of kinematic viscosity from cSt to m^2/s, simply multiply it by 10^{-6}; the kinematic viscosity (m^2/s) can be used to calculate the dynamic viscosity μ (Pa·s) of the lubricant [59],

$$\mu = \rho_{lub} \cdot \nu, \tag{24}$$

and this value can be used to calculate the film thickness using the Hamrock–Dowson [33] empirical equations.

If there is a given friction force that will cause the bearings to seize, and the friction is affected by the ratio of the height of the surface asperities (which follow a normal distribution) over the lubricant film thickness, an accurate equation for L_{10} in revolutions $\log_{10}$ as a function of h_c (m) is realized with Equation (25)

$$log_{10}(L_{10}) \quad = \quad b_1 + b_2 \cdot (\frac{P}{C_{a1}})^{3/10} + b_3 \cdot log(h_c), \tag{25}$$

where h_c (m) is the central film thickness in micrometers. Equation (25) incorporates two separate failure mechanisms, where b_2 is a coefficient for the rolling contact fatigue failure [16–18], and b_3 is a coefficient for the lubricant seizure based on friction (originating from Greenwood–Williams theory [19–26]). The fatigue life theory is an entirely different and independent failure mechanism from lubricant seizure; Equation (25) combines both potential failures into L_{10} to obtain an overall probability of bearing failure during a given revolution.

The calculated value of L_{10} found with Equation (25) closely matches the value of L_{10} found with Equation (1), and is observed to match in Figure 1 for a Timken 29348 roller bearing. The coefficients for this particular design are $b_1 = 18.7598$, $b_2 = -7.6583$, and $b_3 = 0.3086$, and the coefficient of determination R^2 between Equation (1) and Equation (25) is 0.96858, showing an extremely strong match.

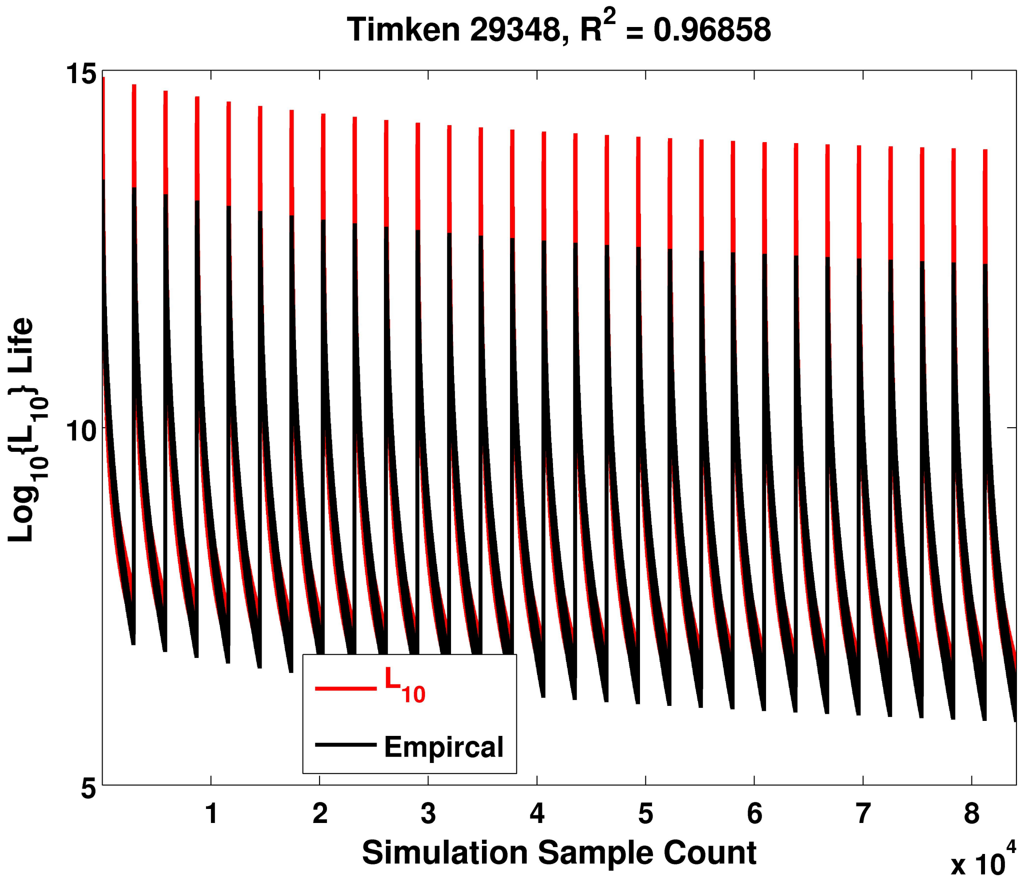

Figure 1. Calculated values of the L_{10} life for the Timken 29348 roller bearing, utilizing theoretical Equation (25) and empirical Equation (1), all for a parametric series of loads, speeds, and lubricant temperatures. The data are placed in the order the parametric sample was conducted on the *X*-axis. The parametric study was conducted for a temperature ranging between 20 °C and 300 °C (112.2355 cSt to 1.0648 cSt), in increments of 10 °C; an equivalent axial load of 1–100% (in 1% increments) of the 2040 kN dynamic load C_{a1}; and a bearing speed of 1000–15,000 RPM, in increments of 500 RPM.

5. Second Parametric Study

A second parametric was conducted to see if varying the bearing size would affect the coefficients for Equation (25), for 52 different spherical roller bearings, with dimensions tabulated in Table 1. The mean bearing radius was modeled from 90 mm to 480 mm. As observed in Figure 2, the three coefficients b_1, b_2, and b_3 vary slightly; the ratio of standard deviation to mean is well under 5%. The average values of the coefficients are $\bar{b}_1 = 18.73$, $\bar{b}_2 = -7.6$, and $\bar{b}_3 = 0.32$; these values are nearly identical to the values found for the Timken 29348 described in Section 4. By plugging these values into Equation (25), a universal equation for the L_{10} failure life for spherical roller bearing life could be obtained, presented as Equation (26). As observed in Figure 3, the coefficient of determination R^2 between this Equation (26) and the Timken equation (Equation (1)) never goes below 0.966, validating this theory of predicted lubricant thickness having a clear and calculable effect on the function life of roller bearings.

$$log_{10}(L_{10}) \quad = \quad 18.73 - 7.6 \cdot (\frac{P}{C_{a1}})^{3/10} + 0.32 \cdot log(h_c). \tag{26}$$

As a simple test, Equation (26) was compared to both the original Timken equation (Equation (1)) [13] and the SKF calculator [14], using the the Timken and SKF 29348 spherical roller thrust bearing, with the Mobil 625 oil (with a kinematic viscosity of 46 cSt at 40 °C, and kinematic viscosity of 8.5 cSt at 100 °C), at a temperature of 70 °C (kinematic viscosity of 15.5429 cSt), a speed of 1,000 RPM, and an axial load of 408 kN (20% of the dynamic fatigue load of 2,040 kN). The calculated $log_{10}(L_{10})$ life with the Timken equation (Equation (1)) was 9.2495; the calculated $log_{10}(L_{10})$ life with Equation (26) was 9.4348, an error of less than 2%. The SKF calculator for the same dimension bearing, with the same speed, load, oil, and temperature, and a simplified lubricant cleanliness factor of 0.6 (middle range between dirtiest of 0.2 and cleanest of 1.0) is 31,700 h, which at 1,000 RPM corresponds to 1.902 billion revolutions; the $log_{10}(L_{10})$ of this value is 9.2792. It is clear that the Timken equation (Equation (1)) [13], the SKF calculator [14], and Equation (26) all yield comparable results, as a further validation of Equation (26).

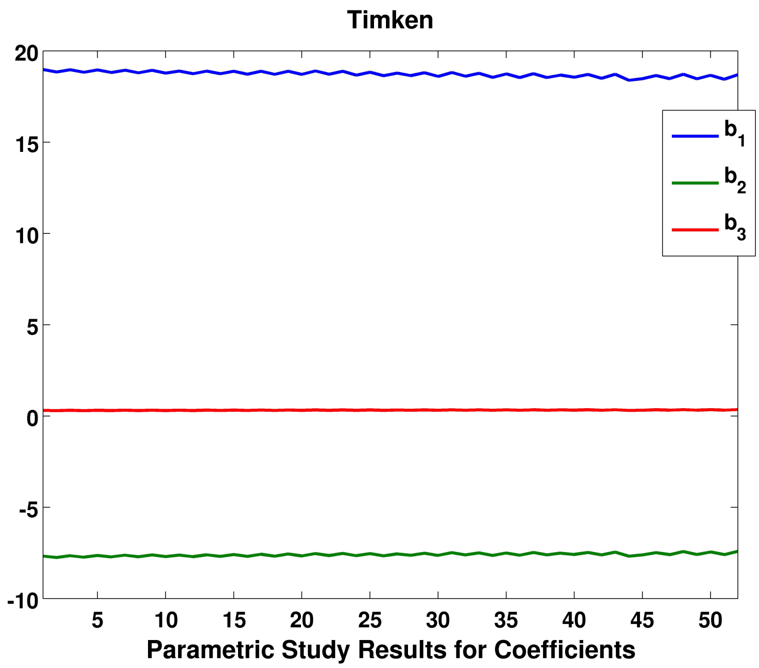

Figure 2. Coefficients of Equation (25), for the 52 different Timken model bearings tabulated in Table 1.

Table 1. Dimensions of Timken Spherical Roller Bearings, used in the parametric study described in Section 5. The average radius of the roller race R_R (m) is the half the average of variables d_b, H, E, and D, where $R_R = \frac{d_b+H+E+D}{8}$.

	Model	d (mm)	C_{a1} (kN)	d_b (mm)	H (mm)	E (mm)	D (mm)
1	29418	90	820	98.9	148	137	190
2	29320	100	462	108.1	141	134	170
3	29420	100	1020	108.8	164	151	210
4	29322	110	604	118.6	157	149	190
5	29422	110	1200	120.3	180	167	230
6	29324	120	768	128.5	172	163	210
7	29424	120	1390	131.6	197	182	250
8	29326	130	852	140.3	186	177	225
9	29426	130	1600	142.4	213	197	270
10	29328	140	970	148.9	199	188	240
11	29428	140	1640	152.8	223	207	280
12	29330	150	993	159.5	209	198	250
13	29430	150	1860	163.5	238	222	300
14	29332	160	1190	170.5	225	213	270
15	29432	160	2100	175	255	237	320
16	29334	170	1230	179.2	235	223	280
17	29434	170	2380	184.8	270	251	340
18	29336	180	1430	190.7	251	238	300
19	29436	180	2660	197.6	286	267	360
20	29338	190	1620	202.2	268	253	320
21	29438	190	3040	205.5	303	281	380
22	29340	200	1880	213.3	284	269	340
23	29440	200	3210	217	317	295	400
24	29344	220	1950	231.6	303	288	360
25	29444	220	3350	237.8	339	317	420
26	29348	240	2040	251.9	323	308	380
27	29448	240	3410	259	360	338	440
28	29352	260	2580	275.7	356	340	420
29	29452	260	4160	279.2	391	367	480
30	29356	280	2580	296.8	376	360	440
31	29456	280	4920	300.6	423	397	520
32	29360	300	3150	315.6	407	388	480
33	29460	300	4990	321.1	443	418	540
34	29364	320	2830	333.3	427	407	500
35	29464	320	5155	320	469	444	580
36	29368	340	3120	365.8	463	443	540
37	29468	340	5922	340	500	473	620
38	29372	360	3632	360	476	457	560
39	29472	360	5440	360	528	498	640
40	29376	380	4295	380	507	486	600
41	29476	380	6493	380	546.1	518	670
42	29380	400	3850	400	534	510	620
43	29480	400	7333	400	577.1	547	710
44	29284	420	2682	420	513.1	498	580
45	29384	420	4040	420	561	537	650
46	29484	420	6780	420	608	576	730
47	29388	440	4530	440	585	561	680
48	29488	440	8606	440	635	602	780
49	29392	460	4820	460	614	589	710
50	29492	460	8120	460	666	631	800
51	29396	480	4820	480	635	610	730
52	29496	480	9320	480	700	662	850

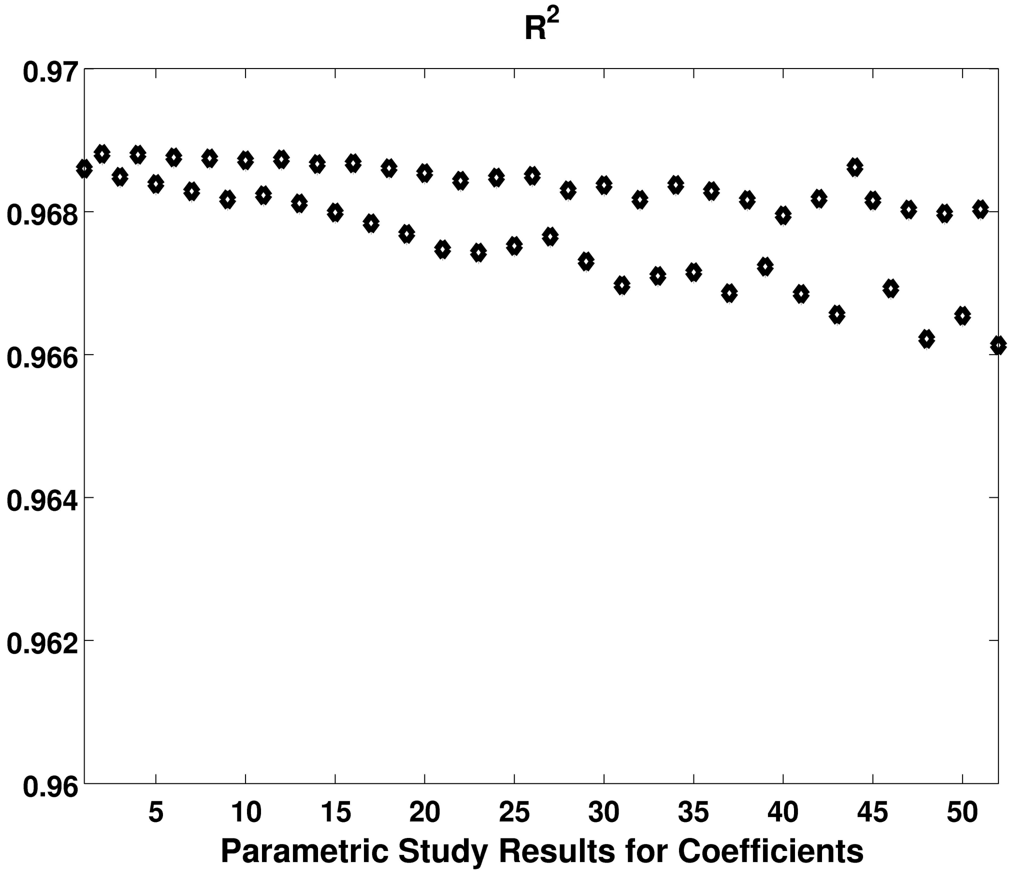

Figure 3. The coefficient of determination R^2 between the calculated values of L_{10} found with Equation (26), as compared to Timken's empirical Equation (1), for the 52 different Timken model bearings tabulated in Table 1.

6. Conclusions

A validated model to predict the probability of failures for roller bearings was developed. Empirical equations from Timken were developed from available data on commercial bearings to predict the L_{10} life based on known bearing conditions (lubricant viscosity, bearing speed, and loads). These conditions were used, along with the roller bearing geometry, to predict the lubricant film thickness at the central point of contact. A thicker film thickness is expected to inherently have lower friction, and therefore a lower chance of lubricant failure, and a clear trend of lubricant thickness impacting the probability of bearing failure per revolution was observed. By knowing the relationship between lubricant film thickness and failure probability, more in-depth analysis of failure can be obtained, such as if one were to numerically solve the Reynolds equation for non-standard geometries, fluctuating temperatures, or rapid accelerations and decelerations. The relative load to the fatigue load is also considered; fatigue is a comparably significant influence on determining the bearing L_{10} life. This model demonstrates how the lubricant film thickness can be used to obtain a reasonable approximation for the life and probability of failure in seizing of a roller bearing.

Supplementary Materials: The supplemenatry materials are available online at https://www.mdpi.com/2075-4442/7/6/48/s1.

Funding: This research was funded by NAVAIR.

Acknowledgments: The author would like to acknowledge Mark Husni and Glenn Shevach for useful discussions.

Conflicts of Interest: The founding sponsors had no role in the design of the study; in the collection, analyses, or interpretation of data; in the writing of the manuscript, and in the decision to publish the results. The author declare no conflict of interest.

Abbreviations

The following abbreviations are used in this manuscript:

L_{10}	Number of revolutions before 10% chance of failure
SKF	Svenska Kullagerfabriken
RMS	Root Mean Square

References

1. Stachowiak, G.; Batchelor, A. *Engineering Tribology*, 4th ed.; Butterworth-Heinemann: Oxford, UK, 2005.
2. Gohar, R. *Elastohydrodynamics*; World Scientific Publishing Company: Singapore, 2002.
3. Ranger, A.; Ettles, C.; Cameron, A. The solution of the point contact elasto-hydrodynamic problem. *Proc. R. Soc. Lond. Ser. A Math. Phys. Sci.* **1975**, *346*, 227–244. [CrossRef]
4. Blau, P. On the nature of running-in. *Tribol. Int.* **2005**, *38*, 1007–1012. [CrossRef]
5. Hu, Y.; Li, N.; Tønder, K. A dynamic system model for lubricated sliding wear and running-in. *J. Tribol.* **1991**, *113*, 499–505. [CrossRef]
6. Suzuki, M.; Ludema, K. The wear process during the "running-in" of steel in lubricated sliding. *J. Tribol.* **1987**, *109*, 587–591. [CrossRef]
7. Endo, K.; Kotani, S. Observations of steel surfaces under lubricated wear. *Wear* **1973**, *26*, 239–251. [CrossRef]
8. Nanbu, T.; Yasuda, Y.; Ushijima, K.; Watanabe, J.; Zhu, D. Increase of traction coefficient due to surface microtexture. *Tribol. Lett.* **2008**, *29*, 105–118. [CrossRef]
9. Wong, P.; Huang, P.; Wang, W.; Zhang, Z. Effect of geometry change of rough point contact due to lubricated sliding wear on lubrication. *Tribol. Lett.* **1998**, *5*, 265–274. [CrossRef]
10. Cann, P.; Spikes, H. In-contact IR spectroscopy of hydrocarbon lubricants. *Tribol. Lett.* **2005**, *19*, 289–297. [CrossRef]
11. Jiang, P.; Li, X.M.; Guo, F.; Chen, J. Interferometry measurement of spin effect on sliding EHL. *Tribol. Lett.* **2009**, *33*, 161–168. [CrossRef]
12. Reddyhoff, T.; Spikes, H.A.; Olver, A.V. Compression heating and cooling in elastohydrodynamic contacts. *Tribol. Lett.* **2009**, *36*, 69–80. [CrossRef]
13. Timken Manual 10424, October 2016. Available online: https://www.timken.com/resources/timken-engineering-manual/ (accessed on 13 April 2019).
14. Svenska Kullager Fabriken AB. SKF Bearing Calculator. 2017. Available online: http://webtools3.skf.com/BearingCalc/selectProduct.action (accessed on 23 April 2019).
15. *SKF Bearing Maintenance Handbook*; SKF Group: Gothenburg, Sweden, 2011; ISBN 978-91-978966-4-1.
16. Zaretsky, E.V. *Rolling Bearing Life Prediction, Theory, and Application*; NASA Technical Report; . Available online: https://ntrs.nasa.gov/search.jsp?R=20160013905 (accessed on 10 September 2018).
17. Zaretsky, E.V. *A. Palmgren Revisited a Basis for Bearing Life Prediction*; NASA Technical Memorandum; Lewis Research Center: Clevelend, OH, USA, 1997. Available online: https://ntrs.nasa.gov/archive/nasa/casi.ntrs.nasa.gov/19970025228.pdf (accessed on 10 September 2018).
18. *Rolling Bearings: Dynamic Load Ratings and Rating Life*; International Organization for Standardization (DIN): Berlin, Germany, 2007. Available online: https://www.iso.org/standard/38102.html (accessed on 10 September 2018).
19. Greenwood, J.; Williamson, J. Contact of nominally flat surfaces. *Proc. R. Soc. Lond. A* **1966**, *295*, 300–319. [CrossRef]
20. Bush, A.; Gibson, R.; Keogh, G. The limit of elastic deformation in the contact of rough surfaces. *Mech. Res. Commun.* **1976**, *3*, 169–174. [CrossRef]
21. Carbone, G. A slightly corrected Greenwood and Williamson model predicts asymptotic linearity between contact area and load. *J. Mech. Phys. Solids* **2009**, *57*, 1093–1102, [CrossRef]
22. McCool, J. Comparison of models for the contact of rough surfaces. *Wear* **1986**, *107*, 37–60. [CrossRef]
23. Bush, A.; Gibson, R.; Thomas, T. The elastic contact of a rough surface. *Wear* **1975**, *35*, 87–111. [CrossRef]
24. Persson, B. Contact mechanics for randomly rough surfaces. *Surf. Sci. Rep.* **2006**, *61*, 201–227. [CrossRef]
25. Finkin, E. Applicability of Greenwood-Williamson theory to film covered surfaces. *Wear* **1970**, *15*, 291–293. [CrossRef]

26. Cann, P.; Ioannides, E.; Jacobson, B.; Lubrecht, A. The lambda ratio—A critical Re-examination. *Wear* **1994**, *175*, 177–188. [CrossRef]
27. Marko, M. Friction of Tungsten-based coatings of steel under sliding contact. *Lubricants* **2019**, *7*, 14. [CrossRef]
28. Crook, A. The lubrication of rollers. *Philos. Trans. R. Soc. Lond. Ser. A Math. Phys. Sci.* **1958**, *250*, 387–409. [CrossRef]
29. Archard, J. The temperature of rubbing surfaces. *Wear* **1958**, *2*, 438–455. [CrossRef]
30. Jaeger, J. Moving sources of heat and the temperature at sliding contact. *Proc. R. Soc. N. S. W.* **1942**, *76*, 203–224.
31. Blok, H. Theoretical study of temperature rise at surfaces of actual contact under oiliness conditions. *Proc. Inst. Mech. Eng. Gen. Discuss. Lubr.* **1937**, *2*, 222–235.
32. Cameron, A.; Gohar, R. Theoretical and experimental studies of the oil film in lubricated point contact. *Proc. R. Soc. Lond. Ser. A Math. Phys. Sci.* **1966**, *291*, 520–536. [CrossRef]
33. Hamrock, B.; Dowson, D. *Isothermal Elastohydrodynamic Lubrication of Point Contacts, III Fully Flooded Results*; NASA Tech. Note; National Aeronautics and Space Administration: Washington, DC, USA, 1976; p. D-8317.
34. Hamrock, B.; Dowson, D. *Isothermal Elastohydrodynamic Lubrication of Point Contacts, I Theoretical Formulation*; NASA Tech. Note; National Aeronautics and Space Administration: Washington, DC, USA, 1975; p. D-8049.
35. Hamrock, B.; Dowson, D. *Isothermal Elastohydrodynamic Lubrication of Point Contacts, IV Starvation Results*; NASA Tech. Note; National Aeronautics and Space Administration: Washington, DC, USA, 1976; p. D-8318.
36. Dowson, D. Elastohydrodynamic and micro-elastohydrodynamic lubrication. *Wear* **1995**, *190*, 125–138. [CrossRef]
37. Nam, J.; Ryou, H.; Cho, S. A numerical model of rotating bearings for thermo-mechanical coupled analysis. *Proc. Int. Conf. Simul. Exp. Heat Transf. Appl.* **2016**, *106*, 25–31. [CrossRef]
38. Lugt, P.M.; Velichov, S.; Tripp, J.H. On the chaotic behavior of grease lubrication in rolling bearings. *Tribol. Trans.* **2009**, *52*, 581–590. [CrossRef]
39. van Zoelen, M.; Venner, C.; Lugt, P. Prediction of film thickness decay in starved elasto-hydrodynamically lubricated contacts using a thin layer flow model. *J. Eng. Tribol.* **2009**, *223*, 541–552. [CrossRef]
40. Venner, C.H.; Popovici, G.; Lugt, P.M.; Organisciak, M. Film thickness modulations in starved elastohydrodynamically lubricated contacts induced by time varying lubricant supply. *ASME J. Tribol.* **2008**, *130*, 041501. [CrossRef]
41. Venner, C.; van Zoelen, M.; Lugt, P. Thin layer flow and film decay modeling for grease lubricated rolling bearings. *Tribol. Int.* **2012**, *47*, 175–187. [CrossRef]
42. Fillot, N.; Berro, H.; Vergne, P. From continuous to molecular scale in modelling elastohydrodynamic lubrication: Nanoscale surface slip effects on film thickness and friction. *Tribol. Lett.* **2011**, *43*, 257–266. [CrossRef]
43. Guo, F.; Wong, P.L.; Geng, M.; Kaneta, M. Occurrence of wall slip in elastohydrodynamic lubrication contacts. *Tribol. Lett.* **2009**, *34*, 103–111. [CrossRef]
44. Krupka, I.; Bair, S.; Kumar, P.; Svoboda, P.; Hartl, M. Mechanical degradation of the liquid in an operating EHL contact. *Tribol. Lett.* **2011**, *41*, 191–197. [CrossRef]
45. Marko, M. The Tribological Effects of Lubricating Oil Containing Nanometer-Scale Diamond Particles. Ph.D. Thesis, Columbia University, New York, NY, USA, 2015. [CrossRef]
46. Marko, M.; Kyle, J.P.; Wang, Y.S.; Terrell, E.J. Tribological investigations of the load, temperature, and time dependence of wear in sliding contact. *PLOS ONE* **2017**, *12*, e0175198. [CrossRef] [PubMed]
47. Marko, M.D.; Kyle, J.P.; Branson, B.; Terrell, E.J. Tribological improvements of dispersed nano-diamond additives in lubricating mineral oil. *J. Tribol.* **2015**, *137*, 011802. [CrossRef]
48. Marko, M.D.; Kyle, J.P.; Wang, Y.S.; Branson, B.; Terrell, E.J. Numerical and experimental tribological investigations of diamond nanoparticles. *J. Tribol.* **2016**, *138*, 032001. [CrossRef]
49. Johnson, K. *Contact Mechanics*; Cambridge University Press: New York, NY, USA, 1987.
50. Einstein, A. Neue Bestimmung der molekuldimensionen. *Ann. Phys.* **1906**, *19*, 289–306. [CrossRef]
51. Pabst, W. Fundamental considerations on suspension rheology. *Ceram. Silik.* **2004**, *48*, 6–13.
52. So, B.; Klaus, E. Viscosity-pressure correlation of liquids. *ASLE Trans.* **1980**, *23*, 409–421. [CrossRef]

53. *ASTM D341-09, Standard Practice for Viscosity-Temperature Charts for Liquid Petroleum Products*; ASTM-International: West Conshohocken, PA, USA, 2009. Available online: www.astm.org (accessed on 21 January 2013).
54. Cengel, Y. *Heat Transfer, a Practical Approach*, 2nd ed.; Mcgraw-Hill: Boston, MA, USA, 2002.
55. Abdel-Aal, H. A remark on the flash temperature theory. *Int. Commun. Heat Mass Transf.* **1997**, *24*, 241–250. [CrossRef]
56. Barber, J. Distribution of heat between sliding surfaces. *J. Mech. Eng. Sci.* **1967**, *9*, 351–354. [CrossRef]
57. Blok, H. The flash temperature concept. *Wear* **1963**, *6*, 483–494. [CrossRef]
58. Archard, J.; Rowntree, R. The temperature of rubbing bodies; Part 2, the distribution of temperatures. *Wear* **1988**, *128*, 1–17. [CrossRef]
59. White, F. *Fluid Mechanics*, 5th ed.; McGraw-Hill: Boston, MA, USA, 2003.